Proton Addition to an Anionic Carbene Complex as a Route to Seven-Coordinate Methyl Carbonyl Complexes in Equilibrium with η^2-Acyl Complexes

Kenneth C. Stone, Adanna Onwuzurike, Peter S. White, and Joseph L. Templeton*

Department of Chemistry, University of North Carolina at Chapel Hill, Chapel Hill, North Carolina 27599-3290

Received April 13, 2004

Proton addition to the anionic methylene carbene complex [Na][Tp′$(CO)_2$W=CH_2] in the presence of a trapping phosphine ligand generates seven-coordinate complexes of the form Tp′$(CO)_2(PR_3)W(CH_3)$ (PR_3 = PMe_3, PMe_2Ph, $PMePh_2$). The seven-coordinate phosphine complexes are in equilibrium with their CO-insertion products Tp′$(CO)(PR_3)W(\eta^2$-C(O)Me). The geometry of these complexes allowed us to probe the stereoselectivity of CO insertion into the W−Me bond by means of a C-13 spin-saturation transfer NMR experiment. The $\Delta G^{\ddagger}_{358}$ value determined for the insertion reaction was 18.5 kcal/mol for the PMe_2Ph adduct. Single-crystal structures revealed detailed solid state geometries for Tp′$(CO)_2(PMe_2Ph)W(CH_3)$, Tp′$(CO)_2(PMe_3)W(CH_3)$, Tp′$(CO)(PMe_3)W(\eta^2$-C(O)$CH_3)$, and a second isomer of Tp′$(CO)_2(PMe_3)W(CH_3)$. Trapping of the protonated carbene complex with phenyl acetylene yields an η^1-acyl product.

Introduction

Anionic carbene complexes are rare relative to neutral and cationic carbene complexes. Reactions of several anionic group VI carbene complexes have been reported during the past decade.[1−11] Protonation at metal followed by hydride migration to a carbene ligand has been observed for the anionic Cp carbene complex [Cp$(CO)_2$Mo=C(κ^2-C,N-$(CH_2)_3$NMe)]$^-$ (**1**), which resulted in the formation of the η^2-alkylamine complex Cp$(CO)_2$Mo(η^2-C,N-CH(κ^2-C,N-$(CH_2)_3$NMe)) (**2**) (Scheme 1).[12] A related migration was observed for the carbene complex Cp$(CO)_2(\eta^1$-C(O)Ph)W=C(κ^2-C,N-$(CH_2)_3$NMe) (**3**), in which the benzoyl ligand migrates to the carbene ligand to form Cp$(CO)_2$W(η^2-C,N-C(κ^2-C,N-$(CH_2)_3$NMe)-(C(O)Ph)) (**4**) (Scheme 2).[9]

The mechanism of carbon monoxide insertion reactions leading to transition metal acyl complexes has long been investigated due to the importance of generating organic products from a CO feedstock.[13,14] Migratory insertion of CO into a transition metal−alkyl bond is

Scheme 1. Formation of an η^2-Alkylamine Ligand from Protonation of an Anionic Carbene Complex

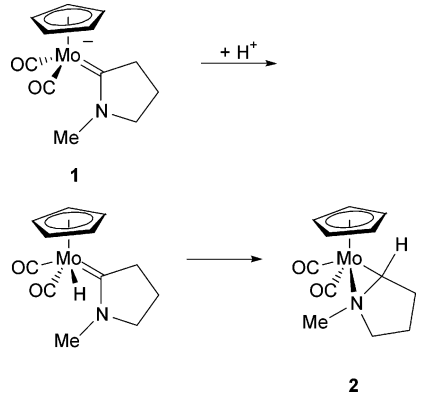

1 2

Scheme 2. Benzoyl−Carbene Coupling by Cp$(CO)_2(\eta^1$-C(O)Ph)W=C(κ^2-C,N-$(CH_2)_3$NMe) (3)

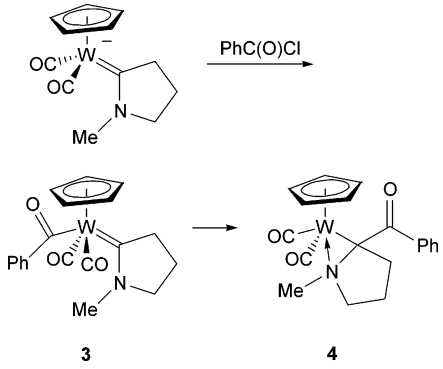

3 4

* Corresponding author. E-mail: joetemp@unc.edu.

(1) Enriquez, A. E.; White, P. S.; Templeton, J. L. *J. Am. Chem. Soc.* **2001**, *123*, 4992.
(2) Legzdins, P.; Sayers, S. F. *Chem. Eur. J.* **1997**, *3*, 1579.
(3) Legzdins, P.; Sayers, S. F. *Organometallics* **1996**, *15*, 3907.
(4) Schrock, R. R.; Luo, S.; Lee, J. C., Jr.; Zanetti, N. C.; Davis, W. M. *J. Am. Chem. Soc.* **1996**, *118*, 3883.
(5) Muir, J. E.; Haynes, A.; Winter, M. J. *Chem. Commun.* **1996**, 1765.
(6) Adams, H.; Bailey, N. A.; Bentley, G. W.; Muir, J. E.; Winter, M. J. *J. Chem. Soc., Chem. Commun.* **1995**, 515.
(7) Adams, H.; Bailey, N. A.; Bentley, G. W.; Tattershall, C. E.; Taylor, B. F.; Winter, M. J. *J. Chem. Soc., Chem. Commun.* **1992**, 533.
(8) Adams, H.; Bailey, N. A.; Winter, M. J.; Woodward, S. *J. Organomet. Chem.* **1991**, *418*, C39.
(9) Adams, H.; Bailey, N. A.; Tattershall, C. E.; Winter, M. J. *J. Chem. Soc., Chem. Commun.* **1991**, 912.
(10) Adams, H.; Bailey, N. A.; Winter, M. J.; Woodward, S. *J. Organomet. Chem.* **1991**, *410*, C21.
(11) Lee, S.; Cooper, N. J. *J. Am. Chem. Soc.* **1990**, *112*, 9419.
(12) Osborn, V. A.; Parker, C. A.; Winter, M. J. *J. Chem. Soc., Chem. Commun.* **1986**, 1185.
(13) Chiusoli, G. P. *Transition Met. Chem.* **1991**, *16*, 553.
(14) Durfee, L. D.; Rothwell, I. P. *Chem. Rev.* **1988**, *88*, 1059.

10.1021/om049725s CCC: $27.50
Publication on Web 07/31/2004

Scheme 3. Reversible Migratory Insertion in Group IV Complexes

Scheme 4. Reversible CO Migratory Insertion in Pd Complexes

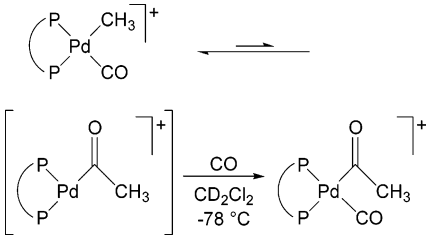

rarely a simple equilibrium transformation.[14] A few group IV transition metal complexes have been investigated in which acyl-incorporated CO was in equilibrium with free CO (Scheme 3).[15−17] A series of Pd CO/olefin copolymerization catalysts with methyl and carbonyl ligands underwent reversible migratory insertion, and the acyl intermediate was trapped by addition of CO (Scheme 4).[18,19] These insightful studies have clarified the details of CO migratory insertion for those systems and thus supplemented definitive investigations of insertion reactions of Mn complexes.[20−22] The kinetics and geometry associated with reversible CO migratory insertion in group VI transition metal-alkyl complexes have received less attention.[23−25]

In exploring electrophilic addition to the anionic carbene complex [Na][Tp′(CO)$_2$W=CH$_2$] (**5**) (Tp′ = hydridotris(3,5-dimethylpyrazolyl)borate),[1] we have now observed that addition of a proton source and a trapping ligand to the carbene complex **5** results in the formation of a methyl ligand poised to insert CO. We report here the synthesis, isolation, and characterization of the η^1-acyl phenylacetylene complex Tp′(CO)(PhC≡CH)W(η^1-C(O)Me) (**6**) (Scheme 5), as well as the seven-coordinate methyl dicarbonyl tungsten complex Tp′(CO)$_2$(PMe$_2$Ph)W(CH$_3$) (**7a**) in equilibrium with the isomeric η^2-acyl complex Tp′(CO)(PMe$_2$Ph)W(η^2-C(O)CH$_3$) (**7b**). A slower isomerization process converts mixtures of chiral **7a** and chiral **7b** to yet a third isomer, a seven-coordinate dicarbonyl methyl tungsten(II) complex with mirror symmetry. Similar results are obtained with closely related phosphine ligands that produce Tp′(CO)$_2$(PMe$_3$)W(CH$_3$) (**8a**) and Tp′(CO)(PMePh$_2$)W(η^2-C(O)CH$_3$) (**9b**).

Scheme 5. Formation of Tp′(CO)(PhC≡CH)W(η^1-C(O)Me) (6)

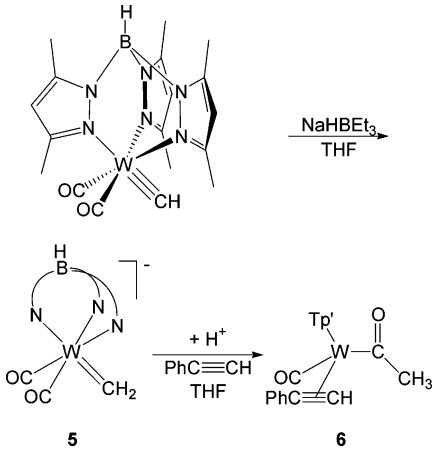

Scheme 6. Formation of Related η^1-Acyl Alkyne Complex Tp′(CO)(PhC≡CMe)W(η^1-C(O)Bu^n) (10)

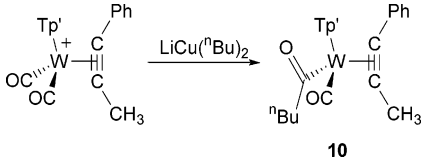

Results and Discussion

***η*^{1}-Acyl Phenylacetylene Complex.** The anionic carbene complex [Na][Tp′(CO)$_2$W=CH$_2$] (**5**) was prepared in situ via addition of Na[HBEt$_3$] to a THF solution of Tp′(CO)$_2$W≡CH at −78 °C.[1] Phenylacetylene was added to the reaction solution; no change was observed in the intensity of the IR absorptions of the anionic carbene complex **5** at 1791 and 1656 cm^{-1}. Addition of acid resulted in new IR absorbance peaks at 1914 and 1782 cm^{-1} as the solution approached room temperature. Chromatography on alumina afforded Tp′(CO)(PhC≡CH)W(η^1-C(O)CH$_3$) (**6**) as a purple solid in 75% yield after solvent removal.

The purple complex Tp′(CO)(PhC≡CH)W(η^1-C(O)CH$_3$) (**6**) is spectroscopically similar to Tp′(CO)(PhC≡CMe)W(η^1-C(O)Bu^n) (**10**), an η^1-acyl alkyne complex made by addition of LiCu(Bu^n)$_2$ to [Tp′W(CO)$_2$(PhC≡CMe)][BF$_4$] (Scheme 6).[26] Downfield proton signals at 13.35 ppm for the major isomer and 12.72 ppm for the minor isomer were assigned to the η^2-phenylacetylene ligand, and resonance signals in the ^{13}C{^{1}H} NMR spectrum of **6** at 216.7 and 200.0 ppm for the two carbons of the acetylene fragment of the major isomer support assignment of the alkyne ligand as a four-electron donor.[27] The acyl ligand of **6** is assigned an η^1-bonding arrangement based on the phenylacetylene ^{13}C{^{1}H} resonances and other NMR data that are similar to data reported for the η^1-acyl complex Tp′(CO)(PhC≡CMe)W(η^1-C(O)Bu^n) (**10**).[26] The two isomers of **6** observed by ^{1}H NMR result from of two orientations of the alkyne ligand, common among tungsten(II) complexes with PhC≡CH in the coordination sphere (Figure 1).[27,28]

(15) Fachinetti, G.; Floriani, C. *J. Organomet. Chem.* **1974**, *71*, C5.
(16) Fachinetti, G.; Fochi, G.; Floriani, C. *J. Chem. Soc., Dalton Trans.* **1977**, 1946.
(17) Marsella, J. A.; Moloy, K. G.; Caulton, K. G. *J. Organomet. Chem.* **1980**, *201*, 389.
(18) Ledford, J.; Shultz, C. S.; Gates, D. P.; White, P. S.; DeSimone, J. M.; Brookhart, M. *Organometallics* **2001**, *20*, 5266.
(19) Shultz, C. S.; Ledford, J.; DeSimone, J. M.; Brookhart, M. *J. Am. Chem. Soc.* **2000**, *122*, 6351.
(20) Stimson, R. E.; Shriver, D. F. *Organometallics* **1982**, *1*, 787.
(21) Flood, T. C.; Jensen, J. E.; Statler, J. A. *J. Am. Chem. Soc.* **1981**, *103*, 4410.
(22) Berry, A.; Brown, T. L. *Inorg. Chem.* **1972**, *11*, 1165.
(23) Ford, P. C.; Ryba, D. W.; Belt, S. T. *Adv. Chem. Ser.* **1993**, *238*, 27.
(24) Jones, W. D.; Huggins, J. M.; Bergman, R. G. *J. Am. Chem. Soc.* **1981**, *103*, 4415.
(25) Wojcicki, A. *Adv. Organomet. Chem.* **1973**, *11*, 87.
(26) Feng, S. G.; Templeton, J. L. *Organometallics* **1992**, *11*, 2168.
(27) Templeton, J. L. *Adv. Organomet. Chem.* **1989**, *29*, 1.
(28) Feng, S. G.; Philipp, C. C.; Gamble, A. S.; White, P. S.; Templeton, J. L. *Organometallics* **1991**, *10*, 3504.

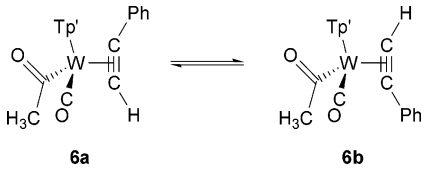

Figure 1. Two isomers of Tp′(CO)(PhC≡CH)W(η^1-C(O)-CH_3) (**6**).

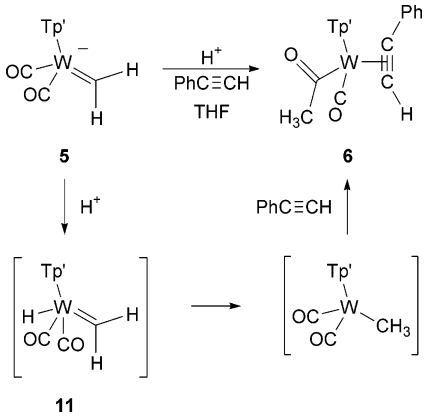

Figure 2. Possible mechanism for the formation of Tp′-(CO)(PhC≡CH)W(η^1-C(O)CH_3) (**6**).

Although direct protonation at the carbene carbon is compatible with the products we isolate, a mechanism similar to that observed for the formation of the η^2-alkylamine complex **2** is attractive for the initial steps in the formation of the alkyne acyl complex **6**.[12] In such a sequence addition of acid to **5** would initially form a carbene-hydride intermediate of the form Tp′$(CO)_2$-(H)W=CH_2 (**11**) (Figure 2) that would quickly undergo hydride migration to the carbene ligand and then insert CO into the resulting tungsten−methyl bond. Coordination of alkyne would form Tp′(CO)(PhC≡CH)W(η^1-C(O)-CH_3) (**6**), the observed product. Note that the recently isolated anionic carbene complex [Et_4N][Tp′$(CO)_2$-Mo=$C(CN)_2$] (**12**)[29] reacts with alkylating reagents neither at the carbon nor at the metal, but rather at the nitrogen atoms of the cyano substituents.[30]

Methyl and η^2-Acyl Phosphine Complexes: Synthesis and Characterization. Formation of the η^1-acyl phenylacetylene complex Tp′(CO)(PhC≡CH)W(η^1-C(O)Me) (**6**) suggested that using a two-electron donor trapping ligand (L) might yield an η^2-acyl complex of the form Tp′(CO)(L)W(η^2-C(O)CH_3). Protonation of anionic carbene **5** and addition of PMe_2Ph at −78 °C in THF solution led to new IR absorbance peaks at 1897 and 1794 cm^{-1} that suggested formation of a neutral dicarbonyl species. The brown solution became orange as the solution warmed to room temperature, and a new absorbance appeared in the IR spectrum at 1777 cm^{-1}. The changes in the IR spectra suggested initial formation of a dicarbonyl intermediate that converted to a monocarbonyl complex. A ^1H NMR spectrum obtained after chromatography revealed the presence of two chiral species in a 6:1 ratio. A 2D NOESY NMR experiment, sensitive to chemical exchange processes, indicated that exchange was occurring between a methyl signal for the major species at 2.79 ppm and a methyl signal at 0.78 ppm for the minor species.

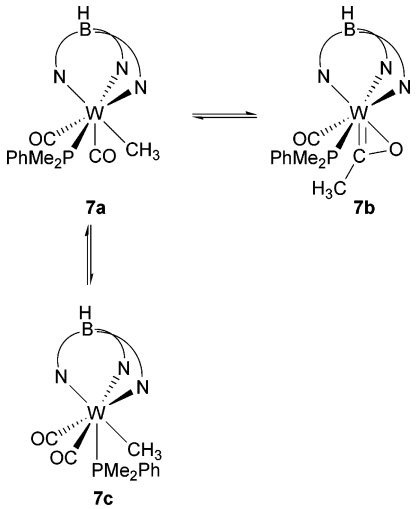

Figure 3. Three isomers of **7** in equilibrium in solution.

Scheme 7. Formation of Methyl Dicarbonyl Complex 7a and η^2-Acyl Complex 7b

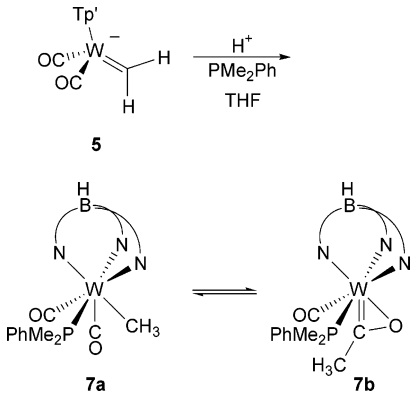

The methyl group of the major species at 2.79 ppm in the ^1H NMR spectrum exhibited coupling to phosphorus of 1 Hz. The methyl group from the minor species at 0.78 ppm exhibited phosphorus coupling of 4 Hz. A cross-peak in the 2D HMBC spectrum probing $^2J_{CH}$ or $^3J_{CH}$ correlations was observed between the proton resonance at 2.79 ppm and a carbene-like resonance at 267.0 ppm. No such correlation was observed for the proton resonance at 0.78 ppm. The NMR and IR data led us to assign the initially formed kinetic product as a seven-coordinate methyl dicarbonyl complex, Tp′$(CO)_2(PMe_2Ph)W(CH_3)$ (**7a**), and the ensuing product as the η^2-acyl complex Tp′(CO)(PMe_2Ph)W-(η^2-C(O)CH_3) (**7b**) (Scheme 7).

The C_s Isomer. During the time required for spectral characterization of the two chiral PMe_2Ph adducts, methyl dicarbonyl complex **7a** and η^2-acyl complex **7b**, signals for a new species with a mirror plane of symmetry slowly emerged in the NMR spectrum. This third product is assigned as a second methyl dicarbonyl isomer, Tp′$(CO)_2(PMe_2Ph)W(CH_3)$ (**7c**). The C_s symmetric complex **7c** reached equilibrium with complexes **7a** and **7b** after about 2 days (**7a**:**7b**:**7c** = 1:6:1, Figure 3), in contrast with the 20 min it took for **7a** to equilibrate with **7b**. Isomerization of **7a** to **7c** is compatible with the shallow energy surface typical of many seven-coordinate complexes, and in fact the rate

(29) Ferguson, G.; Lalor, F. J.; O'Neill, S. A. *Acta Crystallogr.* **2003**, *E59*, m644.
(30) Lalor, F. J.; O'Neill, S. A. *J. Organomet. Chem.* **2003**, *684*, 249.

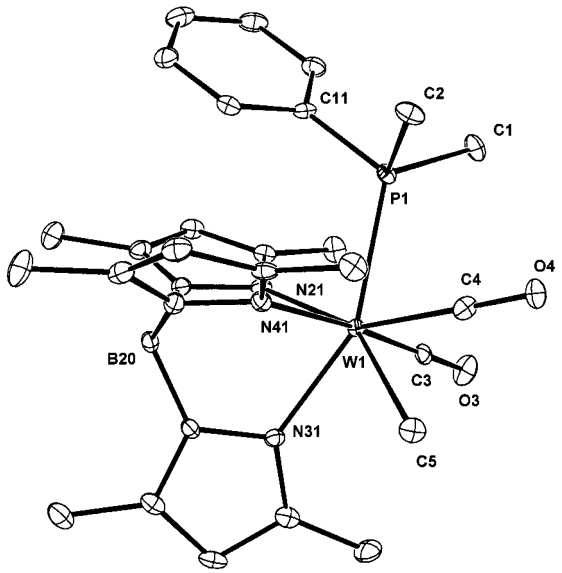

Figure 4. ORTEP representation of C_1 symmetric Tp′-$(CO)_2(PMe_2Ph)W(CH_3)$ (**7a**). C(4) occupies the capped-octahedral site.

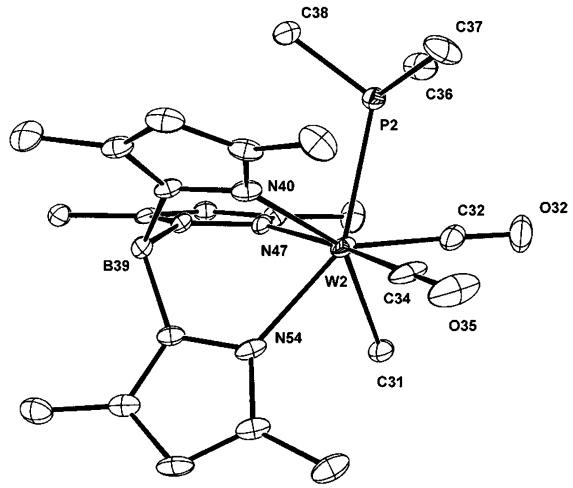

Figure 5. ORTEP representation of C_1 symmetric Tp′-$(CO)_2(PMe_3)W(CH_3)$ (**8a**). C(32) occupies the capped-octahedral site.

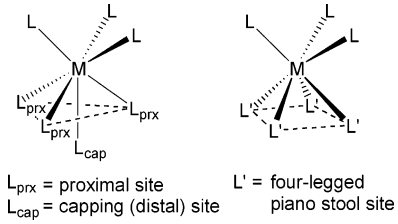

Figure 6. Depiction of capped-octahedral and four-legged piano stool geometries.

of formation of **7c** is surprisingly slow.[31−41] The slow conversion of **7a** and **7b** to **7c** is consistent with assignment of the kinetic product observed during the synthesis of **7** as the chiral dicarbonyl complex **7a**, which forms an equilibrium amount of **7b** as the solution warms to room temperature (vide supra). The higher barrier required to form **7c** relative to the barrier between **7a** and **7b** indicates that the C_s symmetric seven-coordinate complex **7c** is not a kinetically competent intermediate along the reaction path connecting **7a** and **7b**.

Single-Crystal Structure Determinations. The seven-coordinate kinetic products Tp′$(CO)_2(PMe_2Ph)W(CH_3)$ (**7a**) and Tp′$(CO)_2(PMe_3)W(CH_3)$ (**8a**) represent energy minima on the path to η^2-acyl complexes. It is convenient to assign an η^2-bound acyl ligand to a single coordination site in order to simplify structural discussions. Recrystallization of a mixture of **7a**−**c** resulted in orange rods of the methyl dicarbonyl isomer **7a**. Crystalline red blocks formed from a solution of **8a**−**c** allowed determination of the structure of **8a**. The crystal structures of **7a** and **8a** are presented in Figure 4 (Table 1) and Figure 5 (Table 2), respectively.

Two common geometries for seven-coordinate transition metal complexes are capped-octahedron and four-leg piano stool (Figure 6). The complex [Tp′$(CO)_3W(PMe_2Ph)$][PF_6] (**13**) displays a capped-octahedral geometry on the basis of crystal structure and NMR data.[38] An example of a complex that exhibits a four-leg piano stool geometry, commonly observed for complexes bearing Cp ligands, is $Cp(CO)_2(\eta^1$-C(O)Ph)W=C(κ^2-C,N-$(CH_2)_3$NMe) (**3**, vide supra).[9] The complex Tp′$(CO)_2$-

Table 1. Selected Bond Distances (Å) and Bond Angles (deg) for Tp′$(CO)_2(PMe_2Ph)W(CH_3)$ (7a)

Distances (Å)			
W−P(1)	2.502(1)	W−N(31)	2.233(4)
W−C_{Me}(5)	2.35(1)	W−N(21)	2.267(4)
W−C(3)	1.91(1)	W−N(41)	2.293(4)
W−C(4)	1.94(1)	C(4)−C_{Me}(5)	2.15(1)
C(3)−C_{Me}(5)	3.21(1)		
Bond Angles (deg)			
P(1)−W−N(31)	153.4(1)	C(4)−W−N(31)	134.9(2)
C_{Me}(5)−W−N(21)	151.2(1)	C(4)−W−N(21)	149.5(2)
C(3)−W−N(41)	176.0(2)	C(4)−W−N(41)	101.1(2)
C(4)−W−P(1)	71.3(1)	C(4)−W−C_{Me}(5)	59.3(2)
C(4)−W−C(3)	81.8(2)	C_{Me}(5)−W−C(3)	97.3(2)

Table 2. Selected Bond Distances (Å) and Bond Angles (deg) for Tp′$(CO)_2(PMe_3)W(CH_3)$ (8a)

Distances (Å)			
W(2)−P(2)	2.505(2)	W(2)−N(54)	2.27(1)
W(2)−C_{Me}(31)	2.29(1)	W(2)−N(40)	2.27(1)
W(2)−C(34)	1.91(1)	W(2)−N(47)	2.292(4)
W(2)−C(32)	1.95(1)	C(32)−C_{Me}(31)	2.33(1)
C(34)−C_{Me}(31)	3.22(1)		
Bond Angles (deg)			
P(2)−W(2)−N(54)	148.7(1)	C(32)−W(2)−N(54)	138.0(2)
C_{Me}(31)−W(2)−N(40)	148.8(2)	C(32)−W(2)−N(40)	145.2(2)
C(34)−W(2)−N(47)	175.7(2)	C(32)−W(2)−N(47)	107.4(2)
C(32)−W(2)−P(2)	73.0(2)	C(32)−W(2)−C_{Me}(31)	65.8(2)
C(34)−W(2)−C(32)	76.1(3)	C(34)−W(2)−C_{Me}(31)	99.5(2)

(31) Zhu, G.; Tanski, J. M.; Parkin, G. *Polyhedron* **2003**, *22*, 199.
(32) Baker, P. K.; Drew, M. G. B.; Johans, A. W.; Haas, U.; Latif, L. A.; Meeham, M. M.; Zanin, S. *J. Organomet. Chem.* **1999**, *590*, 77.
(33) Szymanska-Buzar, T.; Glowiak, T. *J. Organomet. Chem.* **1999**, *575*, 98.
(34) Barton, R. J.; Manocha, S. K.; Robertson, B. E.; Mihichuk, L. M. *Can. J. Chem.* **1998**, *76*, 245.
(35) Blower, P. J.; Jeffery, J. C.; Miller, J. R.; Salek, S. N.; Schmaljohann, D.; Smith, R. J.; Went, M. J. *Inorg. Chem.* **1997**, *36*, 1578.
(36) Baker, P. K.; Clark, A. I.; Drew, M. G. B.; Durrant, M. C.; Richards, R. L. *J. Organomet. Chem.* **1997**, *549*, 193.
(37) Hughes, D. L.; Lazarowych, N. J.; Maguire, M. J.; Morris, R. H.; Richards, R. L. *J. Chem. Soc., Dalton Trans.* **1995**, 5.
(38) Philipp, C. C.; White, P. S.; Templeton, J. L. *Inorg. Chem.* **1992**, *31*, 3825.
(39) Dewan, J. C.; Roberts, M. M.; Lippard, S. J. *Inorg. Chem.* **1983**, *22*, 1529.
(40) Dewan, J. C.; Lippard, S. J. *Inorg. Chem.* **1982**, *21*, 1682.
(41) Dreyer, E. B.; Lam, C. T.; Lippard, S. J. *Inorg. Chem.* **1979**, *18*, 1904.

$(PMe_2Ph)W(CH_3)$ (**7a**) adopts a capped-octahedral geometry with CO in the capping position (vide supra). For the sake of clarity in this paper, we will divide the ligand sites of the capped-octahedral seven-coordinate $Tp'WL_4$ complexes into three sets: three N-donors from Tp′, three L-donors *cis* to N-donors completing the octahedral framework, and finally one capping ligand, L. We will refer to the ligand coordination sites of the octahedral fragment adjacent to the Tp′ ligand as the "proximal" sites (L_{prx}) and the uniquely positioned L as the capping ligand (L_{cap}) (Figure 6).

Pentagonal-bipyramid or capped-octahedron can both be considered useful descriptions of the geometry of **7a** and **8a**. The axis of a pentagonal-bipyramid can be defined as a line passing near the two ligands with a bond angle closest to 180° about tungsten, here involving a Tp′ pyrazolyl-nitrogen and a carbonyl ligand for both complexes (176° for **7a** and **8a**). The sum of the bond angles between the remaining five ligands, those that define the equatorial belt by default, is 363° for **7a** and 367° for **8a**, with the largest adjacent equatorial bond angle being 81° for **7a** and 79° for **8a**. The validity of the pentagonal-bipyramidal description reflects the unusually close approach of one carbonyl ligand to the methyl ligand.

The capped-octahedral description is the most natural geometry to visualize with the tridentate-Tp′ ligand in the coordination sphere. The octahedral unit can be identified by three bond angles "*trans*" to the Tp′ donor atoms that approach 180°. Each of the Tp′ pyrazolyl-arms defines one end of the three nearly linear bond angles between ligands in **7a** and **8a**. In other words, the Tp′ binding sites are congruent with half an octahedron. The capping element can be defined as the ligand nearest a pseudo-C_3 axis of symmetry created by the octahedral fragment and passing through the Tp′ B−H bond. The carbonyl ligand not included in the canonical octahedral arrangement satisfies this requirement in both **7a** and **8a**. The capping carbonyl ligand in **7a** and **8a** displays roughly equal angles to the three adjacent ligands in each complex, a feature that is inconsistent with a four-leg piano stool description.

Recrystallization of a mixture of **8a**−**c** resulted in two kinds of crystals. Red blocks consisting of a unit cell containing both the methyl dicarbonyl complex **8a** (vide supra) and the η^2-acyl complex $Tp'(CO)(PMe_3)W(\eta^2\text{-}C(O)CH_3)$ (**8b**) (Figure 7, Table 3) and orange needles consisting of the C_s symmetric methyl dicarbonyl complex $Tp'(CO)_2(PMe_3)W(CH_3)$ (**8c**) (Figure 8, Table 4) were formed. The structure of the η^2-acyl complex **8b** is best described as a pseudo-octahedron with the η^2-acyl ligand, assigned as occupying a single coordination site, oriented perpendicular to the carbonyl ligand. The structure of the methyl dicarbonyl complex **8c** possessing C_s symmetry is best described as capped-octahedral with the phosphine ligand in the capping site.

Trapping the $Tp'(CO)_2W(Me)$ Intermediate. The anionic carbene complex $[Na][Tp'(CO)_2W{=}CH_2]$ (**5**), isoelectronic with $[Tp'W(CO)_3]^-$, is expected to possess an octahedral geometry similar to $[Et_4N][Tp'(CO)_2Mo{=}C(CN)_2]$ (**14**).[29] Protonation of **5** at the metal would generate an electronically saturated seven-coordinate intermediate, $Tp'(CO)_2(H)W{=}CH_2$ (**11**) (cf. $Tp'(CO)_2HW(CO)$[42]). Migration of the hydride ligand to the carbene carbon in intermediate **11** would generate an open coordination site, accessible to the phosphine trapping ligand (Figure 9). Solvent binding or agostic interactions may influence the geometry of the unsaturated intermediate.

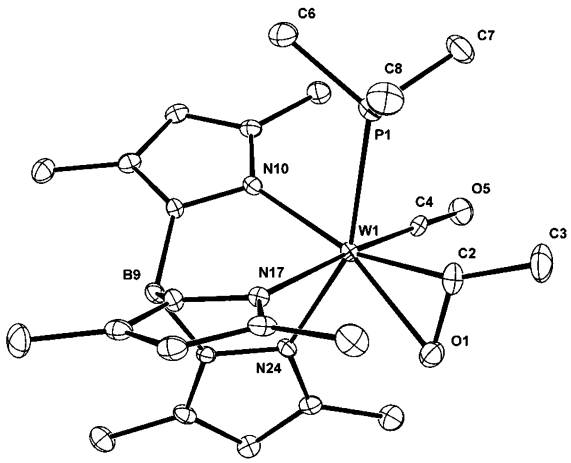

Figure 7. ORTEP representation of $Tp'(CO)(PMe_3)W(\eta^2\text{-}C(O)CH_3)$ (**8b**).

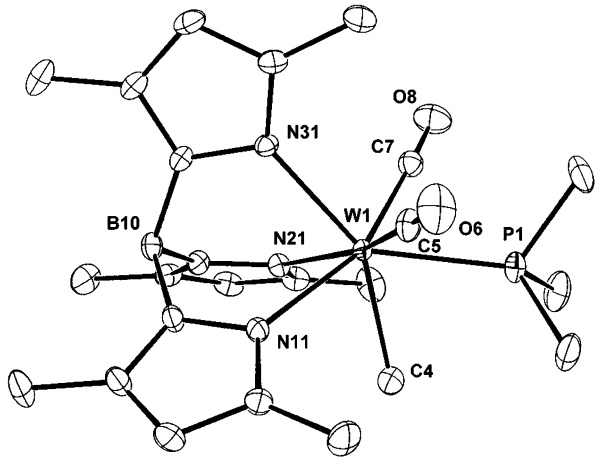

Figure 8. ORTEP representation of C_s symmetric $Tp'(CO)_2(PMe_3)W(CH_3)$ (**8c**). P(1) occupies the capped-octahedral site.

Table 3. Selected Bond Distances (Å), Bond Angles (deg), and Torsion Angles (deg) for $Tp'(CO)(PMe_3)W(\eta^2\text{-}C(O)CH_3)$ (8b)

Distances (Å)			
W−P(1)	2.499(1)	W−N(24)	2.201(4)
W−O(1)	2.206(3)	W−N(10)	2.215(4)
W−C(4)	1.90(1)	W−N(17)	2.304(4)
W−C(2)	1.98(1)	C(2)−C(3)	1.50(1)
C(2)−O(1)	1.29(1)		
Bond Angles (deg)			
P(1)−W−N(24)	157.4(1)	C(2)−W−N(24)	119.4(2)
O(1)−W−N(10)	162.8(1)	C(2)−W−N(10)	161.8(2)
C(4)−W−N(17)	176.1(2)	C(2)−W−N(17)	93.3(2)
C(2)−W−P(1)	81.6(2)	C(2)−W−O(1)	35.3(2)
C(2)−W−C(4)	85.0(2)	W−C(2)−C(3)	158(1)
O(1)−W−C(4)	91.7(2)	W−C(2)−O(1)	82.0(3)
Torsion Angles (deg)			
C(4)−W−C(2)−O(1)		100.1(6)	

(42) Caffyn, A. J. M.; Feng, S. G.; Dierdorf, A.; Gamble, A. S.; Eldredge, P. A.; Vossen, M. R.; White, P. S.; Templeton, J. L. *Organometallics* **1991**, *10*, 2842.

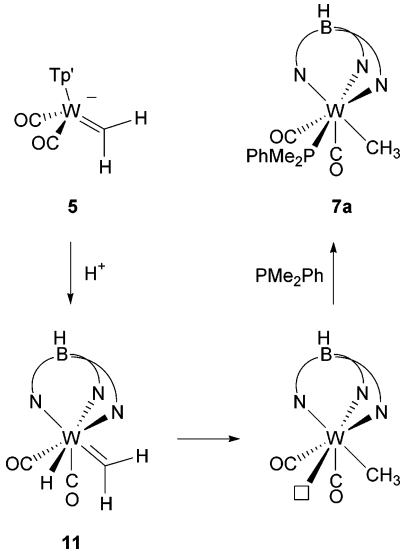

Figure 9. Proposed reaction path leading to an open coordination site.

Table 4. Selected Bond Distances (Å) and Bond Angles (deg) for Tp′(CO)$_2$(PMe$_3$)W(CH$_3$) (8c)

	Distances (Å)		
W−C$_{Me}$(4)	2.23(1)	W−N(31)	2.259(2)
W−C(5)	1.956(3)	W−N(21)	2.282(2)
W−C(7)	1.98(1)	W−N(11)	2.263(2)
W−P(1)	2.435(1)	C(5)−C$_{Me}$(4)	3.46(1)
C(7)−C$_{Me}$(4)	3.56(1)		
	Bond Angles (deg)		
C$_{Me}$(4)−W−N(31)	150.6(2)	P(1)−W−N(31)	137.4(1)
C(5)−W−N(21)	162.1(1)	P(1)−W−N(21)	126.7(1)
C(7)−W−N(11)	158.9(2)	P(1)−W−N(11)	130.1(1)
C$_{Me}$(4)−W−P(1)	72.0(2)	P(1)−W−C(5)	71.2(1)
C$_{Me}$(4)−W−C(5)	111.1(2)	P(1)−W−C(7)	71.0(2)
C$_{Me}$(4)−W−C(7)	115.5(3)		

Reversible Migratory Insertion of CO into a W−Me Bond. The methyl and η^2-acyl dimethylphenylphosphine complexes **7a**−**c** each possess a distinct resonance for the unique methyl group in the ^{1}H NMR spectrum: 1.13 ppm for **7a**, 2.66 ppm for **7b**, and −0.01 ppm for **7c** (in C_6D_5Br at 20 °C). A ^{1}H spin-saturation transfer experiment[43−46] at 75 °C (C_6D_5Br) in which the methyl signal at 2.66 ppm (**7b**) was saturated resulted in almost complete attenuation of the signal at 1.13 ppm (**7a**), while the signal at −0.01 ppm (**7c**) was unaffected. The independence of the methyl signal at −0.01 ppm (**7c**) indicates that neither **7a** nor **7b** provides access to the C_s symmetric isomer **7c** on the NMR time scale under these conditions. Isomers **7a** and **7b** both retained their geometric integrity (a 1:1:1 pattern for the three arms of Tp′) at 85 °C.

The methyl and η^2-acyl dimethylphenylphosphine complexes **7a**−**c** possess a total of five distinct carbonyl resonance peaks in the ^{13}C NMR spectrum (C_6D_5Br at 66 °C): 245.1 and 226.5 ppm (**7a**), 265.1 and 233.4 ppm (**7b**), and 250.4 ppm (**7c**) (Figure 10a). These signals were assigned on the basis of 2D HMBC, relative peak intensities, and separate ^{13}C NMR characterization of isolated **7c** (vide infra). A ^{13}C spin-saturation experiment in which the resonance peak at 265.1 ppm (**7b**) was saturated resulted in attenuation of the signal at 245.1 ppm (**7a**), while the other peaks were unaffected (Figure 10b). Saturation of the peak at 250.4 ppm (**7c**) did not affect the other signals (Figure 10c), and saturation of the peak at 233.4 ppm (**7b**) resulted in attenuation of the peak at 226.5 ppm (**7a**) (Figure 10d). The ^{13}C spin-saturation experiment reveals that only one of the two distinct carbonyl ligands in **7a** inserts into the tungsten−methyl bond, but the spin-saturation experiment alone does not identify which of the two carbonyl ligands participates in migratory insertion. NMR data were correlated with X-ray structural data to map carbonyl resonance peaks in the ^{13}C NMR with each of the two carbonyl ligand sites in the capped-octahedral reagent. One CO occupies a proximal site (near the Tp′ donor atoms of a capped-octahedron) and one a capping (distal) site in **7a**.

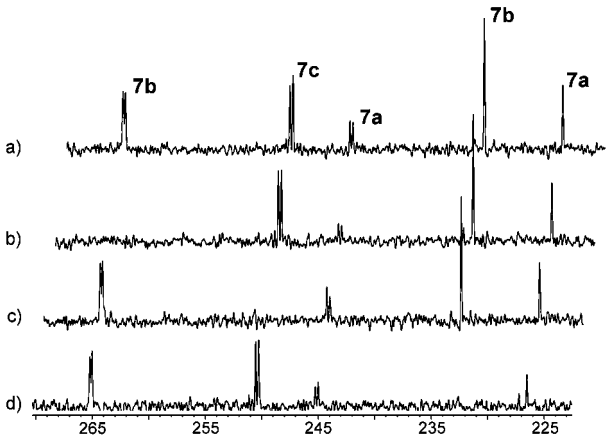

Figure 10. ^{13}C NMR spectra from spin-saturation of carbonyl carbons in **7**: (a) ^{13}C NMR at 66 °C in C_6D_5Br; (b) saturation at 265.1 ppm; (c) saturation at 250.4 ppm; (d) saturation at 233.4 ppm.

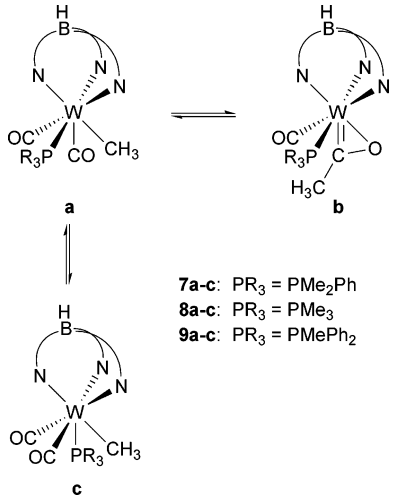

Figure 11. Complexes of the general form Tp′(CO)$_2$(PR$_3$)W(Me) (**7**−**9**).

Relating Structural Data to NMR Data. The ^{13}C NMR data and structural data used to assign carbonyl resonance peaks are summarized in Figure 11 and Table 5. The structure of **7a** is best described as a capped-octahedron in which one of the carbonyl ligands occupies the capping (distal) site (Figure 4, Table 1). The angle between the proximal site phosphine ligand and the

(43) Mann, B. E. *J. Magn. Reson.* **1976**, *21*, 17.
(44) Dahlquist, F. W.; Longmuir, K. J.; DuVernet, R. B. *J. Magn. Reson.* **1975**, *17*, 406.
(45) Forsen, S.; Hoffman, R. A. *J. Chem. Phys.* **1964**, *40*, 1189.
(46) Forsen, S.; Hoffman, R. A. *J. Chem. Phys.* **1963**, *39*, 2892.

Table 5. ^{13}C NMR and ∠P−W−C Structure Data for the Carbonyl Ligands in Complexes 7a−c, 8a−c, and 9b

complex	δ ($^2J_{PC}$, Hz)[a] acyl-^{13}CO	δ ($^2J_{PC}$, Hz)[a] proximal-^{13}CO	∠P−W−C (deg) proximal-CO	δ ($^2J_{PC}$, Hz)[a] capping-^{13}CO	∠P−W−C (deg) capping-CO
7a		227.4(4), 226.5(4)	95	246.5(33), 245.1(32)	71
7b	267.0(26), 265.1(25)	234.7(4), 233.4(4)			
7c		251.4(34), 250.4(34)			
8a		227.9(4)	100	246.3(34)	73
8b	267.1(26)	234.3(4)	92		
8c		250.1(36)	72[b]		
9b	267.6(26)	237.3(4)			

[a] In CD_2Cl_2. If present, the second chemical shift was observed from a sample in C_6D_5Br at 66 °C. [b] Average of two values.

proximal site carbonyl ligand (∠P_{prx}−W−C_{prx}) in **7a** is 95.3(1)°, and the angle between the proximal site phosphine ligand and the capping site carbonyl ligand (∠P_{prx}−W−C_{cap}) is 71.3(1)°. The structure of the methyl dicarbonyl complex **8a** is similar to **7a** (Figure 5, Table 2), and the structure of η^2-acyl complex **8b** (Figure 6, Table 3) is best described as pseudo-octahedral. The structure the C_s symmetric methyl dicarbonyl complex **8c** (Figure 7, Table 4) was also obtained and is best described as capped-octahedral. The ∠P_{prx}−W−C_{prx} and ∠P_{prx}−W−C_{cap} bond angles in **8a** were found to be 100.1(2)° and 73.0(2)° (Table 3), respectively, while **8b** possessed a ∠P−W−C angle of only 91.7(2)°. The two ∠P_{cap}−W−C_{prx} angles in **8c** were determined to be 72°. The key to relating carbonyl ligands in the crystal structure to the carbonyl resonance peaks in the NMR is correlating the phosphine−carbonyl bond angle to the $^2J_{PC}$ coupling constant between the phosphine phosphorus and the carbonyl carbons.

With CD_2Cl_2 as the solvent for $^{13}C\{^1H\}$ NMR, the η^2-acyl carbonyl resonance peak was unambiguously assigned at 267.0 ppm (d, $^2J_{PC}$ = 26 Hz) for **7b** (**8b** 267.1 ppm, d, $^2J_{PC}$ = 26 Hz) on the basis of an HMBC correlation to the methyl proton resonance peak at 2.79 ppm for **7b** (**8b** 2.81 ppm). The carbonyl carbon resonance peaks in the ^{13}C NMR (C_6D_5Br at 66 °C) spectrum at 245.1 (d, $^2J_{PC}$ = 32 Hz) and 226.5 (d, $^2J_{PC}$ = 4 Hz) ppm (**7a**) relative to those at 265.1 (d, $^2J_{PC}$ = 26 Hz) and 233.4 (d, $^2J_{PC}$ = 4 Hz) ppm (**7b**) appear in about a 1:2 ratio, consistent with the **7a**:**7b** ratio determined by ^{1}H NMR in the same solvent at the same temperature.

The remaining carbonyl resonance peak in the ^{13}C NMR (C_6D_5Br at 66 °C) spectrum at 250.4 ppm (d, $^2J_{PC}$ = 34 Hz) was assigned to the C_s symmetric complex **7c** on the basis of its similarity to the resonance at 250.1 ppm (d, $^2J_{PC}$ = 36 Hz) in the $^{13}C\{^1H\}$ NMR (CD_2Cl_2 at 21 °C) spectrum of the C_s symmetric PMe_3 methyl dicarbonyl complex Tp′$(CO)_2(PMe_3)W(CH_3)$ (**8c**) in a sample with low concentrations of the C_1 symmetric complexes Tp′$(CO)_2(PMe_3)W(CH_3)$ (**8a**) and Tp′(CO)-$(PMe_3)W(\eta^2$-C(O)$CH_3)$ (**8b**). The PMe_3 complexes **8a**−**c** were spectroscopically similar to the PMe_2Ph adducts.

The bond angle between a proximal site and a capping site for these complexes was consistently found to be 71−73°, independent of which ligand (carbonyl or phosphine) occupied the capping site. The bond angle between a phosphine ligand and a carbonyl ligand in adjacent proximal sites was 92−100°. Complexes **7b** and **8b** both possess only pseudo-octahedral ∠P−W−C angles, and the lone carbonyl ligand carbon possesses a $^2J_{PC}$ of 4 Hz in both complexes. Complex **8c** possesses only acute ∠P_{cap}−W−C_{prx} bond angles, and the average $^2J_{PC}$ was 36 Hz. On the basis of the correlation between bond angle, ligand binding sites, and phosphorus−carbon coupling constants, the carbon resonance peaks near 245−247 ppm for **7a** and **8a** with $^2J_{PC}$ of 32−34 Hz were assigned to the carbonyl ligand occupying a capping site with a ∠P_{prx}−W−C_{cap} of 71−73°. The carbon resonance peaks near 227−237 ppm for **7b** and **8b** with $^2J_{PC}$ of 4 Hz were consistent with carbonyl ligands occupying proximal sites with a ∠P_{prx}−W−C_{prx} of 95−100° (Table 6). The assignment of the $^2J_{PC}$ of 32−36 Hz to the carbonyl carbon forming an acute ∠P_{cap}−W−C_{prx} or ∠P_{prx}−W−C_{cap} angle of 71−73° is consistent with data for the carbonyl ligands in the phosphine complex [Tp′$(CO)_3W(PMe_2R)$][PF_6] (**13a**, R = Ph; **13b**, R = Me) that possessed an average $^2J_{PC}$ of 33−34 Hz and a ∠P_{cap}−W−C_{prx} of 70−72°.[38] The assignment of the $^2J_{PC}$ of 4 Hz to the carbonyl carbon forming a ∠P−W−C of 92−100° is consistent with the terminal carbonyl ligand in Tp(CO)$(PMe_2Ph)W(\eta^2$-(C,C)-O=C−C-Tol) (**15**) that appeared as a doublet ($^2J_{PC}$ = 4 Hz) in the $^{13}C\{^1H\}$ NMR spectrum. The ∠P−W−C for **15** would be expected to be similar to the 93.0(3)° angle that was found for Tp(CO)$(PMe_2Ph)W(\eta^2$-(C,C)-Se=C−C-Tol) (**16**) in the solid state.[47,48] Phosphine coupling was not observed for the terminal carbonyl ligand carbon in the selenoketenyl complex **16**.

Table 6. ∠P−W−C (deg) and $^2J_{PC}$ (Hz) Data for the Carbonyl Ligands in Complexes 7a and 8a−c

complex	∠P−W−C (deg)	$^2J_{PC}$ (Hz)
7a	95	4
8a	100	4
8b	92	4
7a	71	32
8a	73	34
8c	72	36

The ^{13}C spin-saturation experiments in C_6D_5Br at 66 °C with complexes **7a**−**c** revealed that the carbon that appeared at 245.1 ppm (**7a**) exchanged with the carbon that appeared at 265.1 ppm (**7b**). Therefore, the carbonyl ligand in the capping site in **7a** is the one that undergoes migratory insertion into the tungsten−methyl bond to form the η^2-acyl carbonyl ligand of **7b** (Figure 12). This outcome is consistent with the X-ray structures of **7a** and **8a** since the distance between the carbonyl carbon occupying the capping site and the methyl carbon (**7a** C_{cap}−C_{Me} = 2.15(1) Å, **8a** C_{cap}−C_{Me} = 2.33(1) Å) is about 1 Å shorter than the distance between the carbonyl carbon occupying the proximal site and the methyl carbon (**7a** C_{prx}−C_{Me} = 3.21(1) Å, **8a** C_{prx}−C_{Me} = 3.22(1) Å). This result suggests that a seven-coordinate W(II) complex with capped-octahedral ge-

(47) Baxter, I.; Hill, A. F.; Malget, J. M.; White, A. J. P.; Williams, D. J. *Chem. Commun.* **1997**, 2049.
(48) Hill, A. F., Personal communication.

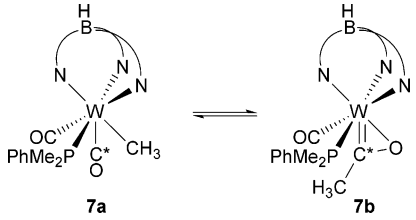

Figure 12. The CO ligand in the capping site in **7a** becomes the acyl carbonyl in **7b**.

ometry can undergo facile insertion if a CO ligand occupies the capping site and the methyl ligand is in an adjacent proximal site.

Kinetic Studies of Migratory Insertion. The kinetics associated with the migratory insertion of CO into the tungsten−methyl bond in Tp′(CO)$_2$(PMe$_2$Ph)W(CH$_3$) (**7a**) to form Tp′(CO)(PMe$_2$Ph)W(η^2-C(O)CH$_3$) (**7b**) were investigated by monitoring line broadening in the ^{1}H NMR spectrum as the temperature of a solution of **7** in C$_6$D$_5$Br was increased. The peaks broadened such that at 85 °C rates of 38 s^{-1} were calculated for **7a** converting to **7b** (k_1, migratory insertion of CO) and 20 s^{-1} for **7b** converting to **7a** (k_{-1}, deinsertion of CO).[49] The ratio of k_1/k_{-1} is 1.9, which is close to the K_{eq}([**7b**]/[**7a**]) value of 2.2 determined by integration of the ^{1}H NMR spectrum at 85 °C. The $\Delta G^{\ddagger}_{358}$ values for interconverting **7a** and **7b** determined from the Eyring equation are 18.5 kcal/mol for k_1 and 19.0 kcal/mol for k_{-1}. The activation parameters determined for an iron system with similar ancillary ligands were $\Delta H^{\ddagger} = 19(1)$ kcal/mol and $\Delta S^{\ddagger} = -20(3)$ cal/mol·K for the conversion of a methyl dicarbonyl reagent to the acyl complex (C$_9$H$_7$)(CO)(PPh$_3$)Fe(COCH$_3$).[50] The $\Delta G^{\ddagger}$ barrier for migratory insertion of CO into a palladium−alkyl bond was found to be in the range 13−18 kcal/mol for the Pd(II) olefin-CO copolymerization catalysts with bidentate phosphine ligands.[18]

Modification of the Phosphine Ligand. Variation of the trapping phosphine ligand had a large influence on the distributions of the isomers present in solution. The PMe$_2$Ph adducts **7a**−**c** were present in a 1:6:1 ratio of the unsymmetrical dicarbonyl isomer (**7a**), the η^2-acyl isomer (**7b**), and the C_s symmetric dicarbonyl isomer (**7c**), respectively. Decreasing the steric bulk of the phosphine ligand by utilizing PMe$_3$ resulted in an increase in the concentration of the C_s symmetric isomer (**8c**) and a decrease of the η^2-acyl isomer (**8b**) such that the ratio was 1:4:8 for **8a**−**c**, respectively. Increasing the steric bulk of the phosphine ligand by utilizing PMePh$_2$ resulted in an increase in the concentration of the η^2-acyl isomer (**9b**) such that only trace amounts of the C_1 and C_s symmetric dicarbonyl isomers (**9a** and **9c**, respectively) were observed in solution. The trend favoring the η^2-acyl isomer with increasing phosphine ligand cone angle may result from steric repulsion in the seven-coordinate methyl dicarbonyl complexes, which is relieved by CO/CH$_3$ coupling.

Conclusion

Seven-coordinate methyl complexes prepared by protonation of the anionic methylidene complex [Na][Tp′(CO)$_2$W=CH$_2$] in the presence of a trapping ligand adopt a capped-octahedral geometry. The CO ligand bound in the capping site along the C_{3v} axis of the Tp′ ligand participated in migratory insertion into the tungsten(II)−methyl bond, while the adjacent CO ligand did not insert into the tungsten−methyl bond. The barrier to CO migratory insertion was found to be 18.5 kcal/mol at 85 °C for Tp′(CO)$_2$(PMe$_2$Ph)W(CH$_3$) (**7a**) on the basis of NMR line broadening experiments. Increasing the cone angle of the phosphine ligand by switching from PMe$_3$ to PMe$_2$Ph to PMePh$_2$ favored the η^2-acyl isomer. Slow rearrangement to an isomer with phosphine in the capping site resulted in a second geometry for the seven-coordinate complex.

Experimental Section

All reactions were run under dry argon or nitrogen with the use of standard Schlenk techniques unless otherwise noted. Solvents, phenylacetylene, and phosphines were used as obtained or dried under nitrogen or argon by molecular sieves, CaH$_2$, P$_2$O$_5$, sodium/benzophenone, or activated alumina columns. Tp′(CO)$_2$W≡CH was prepared according to literature methods.[1] All other reagents were used as obtained from commercial sources. Infrared spectra were obtained with an ASI ReactIR 1000 FTIR spectrometer. ^{1}H and ^{13}C{^{1}H} NMR spectra were recorded on a Bruker DRX-500, a Bruker Avance 400WB, a Bruker DRX-400, or a Bruker AMX-300 spectrometer. Gradient COSY, HMQC, and HMBC 2D NMR were recorded on the DRX-500 or the Avance 400WB. Elemental analyses were performed by Atlantic Microlab, Inc., Norcross, GA.

Tp′(CO)(PhC≡CH)W(η^1-C(O)CH$_3$) (6). A yellow THF solution (25 mL) of Tp′(CO)$_2$W≡CH (301 mg, 0.545 mmol) was cooled to −78 °C with a dry ice−2-propanol bath before [Na][HBEt$_3$] in THF (1.4 mL, 1.4 mmol) was added to the stirring solution. An IR spectrum of the brown solution revealed broad absorbance peaks (1789, 1654 cm^{-1}) that reflected formation of the anionic carbene complex [Na][Tp′(CO)$_2$W=CH$_2$] from the starting material (1987, 1893 cm^{-1}). Phenylacetylene (0.48 mL, 4.36 mmol, 8 equiv) was added to the stirring solution at −78 °C. Addition of HCl (1.0 mL, 1.04 mmol) and warming the solution to room temperature resulted in an IR spectrum with absorbance peaks at 1914, 1582 cm^{-1}. The purple residue remaining after solvent removal was chromatographed on alumina and eluted with CH$_2$Cl$_2$ and 5:1 CH$_2$Cl$_2$/THF. A purple solid consisting of **6** (0.268 g, 75% yield) remained after solvent removal. Two isomers (**6a**:**6b** = 4:1) were observed by NMR. IR (THF): 1914, 1582 cm^{-1} (ν_{CO}). **6a**: ^{1}H NMR (CD$_2$Cl$_2$, RT): δ 13.35 (s, $^2J_{WH}$ = 4 Hz, PhC≡C*H*), 7.28, 6.94 (m, 3:2 H, *Ph*C≡CH), 5.902, 5.896, 5.67 (s, 1:1:1 H, Tp′C*H*), 2.56, 2.46, 2.43, 2.38, 1.49, 1.40 (s, Tp′C*H*$_3$), 1.83 (br s, 3 H, WC(O)C*H*$_3$). ^{13}C{^{1}H} NMR (CD$_2$Cl$_2$, RT): δ 292.3 (br s, W*C*(O)CH$_3$), 237.1 (s, $^1J_{WC}$ = 135 Hz, W*C*O), 216.7 (s, Ph*C*≡CH), 200.0 (s, PhC≡*C*H), 153.9, 148.0, 145.4, 145.3, 144.8 (s, 2:1:1:1:1 C, Tp′*C*CH$_3$), 136.9, 130.6, 129.8, 128.9 (s, 1:2:1:2 C, *Ph*C≡CH), 108.2, 107.9, 106.8 (s, Tp′*C*H), 58.6 (WC(O)*C*H$_3$), 16.5, 15.9, 15.7, 13.1, 13.0, 12.5 (s, Tp′C*C*H$_3$). **6b**: ^{1}H NMR (CD$_2$Cl$_2$, RT): δ 12.72 (br s, PhC≡C*H*), 8.02, 7.64, 7.53 (m, 2:2:1 H, *Ph*C≡CH), 6.11, 5.91, 5.70 (s, 1:1:1 H, Tp′C*H*), 2.53, 2.44, 2.38, 2.19, 1.53, 1.42 (s, Tp′C*H*$_3$), 1.76 (br s, 3 H, WC(O)C*H*$_3$). Anal. Calcd for C$_{26}$H$_{31}$N$_6$BO$_2$W·0.5C$_4$H$_8$O: C, 48.72; H, 5.11; N, 12.17. Found: C, 48.84; H, 5.16; N, 11.92.

Tp′(CO)$_2$(PMe$_2$Ph)W(CH$_3$) (C_1) (7a). The anionic carbene **5** was prepared from Tp′(CO)$_2$W≡CH (300 mg, 0.545 mmol) in the manner described for complex **6**. Addition of PMe$_2$Ph (0.23 mL, 1.6 mmol) caused absorbences to appear at 1897, 1794 cm^{-1} in the IR spectrum. Addition of HCl in Et$_2$O (1.0 mL, 1.0 mmol) resulted in the appearance of a new species (1777 cm^{-1}, minor) that was later assigned to the η^2-acyl

(49) Sandstrom, J. *Dynamic NMR Spectroscopy*; Academic Press: London, 1982.
(50) Monti, D.; Bassetti, M. *J. Am. Chem. Soc.* **1993**, *115*, 4658.

complex Tp′(CO)(PMe_2Ph)W(η^2-C(O)CH_3) (**7b**). The solution was allowed to warm to room temperature, and an IR spectrum revealed that the major absorbance peak was at 1777 cm^{-1}. Solvent was removed in vacuo before the orange residue was chromatographed on alumina under N_2 with dry solvent (first CH_2Cl_2, then 20:1 CH_2Cl_2/THF). Solvent from the orange band was removed in vacuo before the orange residue was recrystallized from Et_2O and CH_2Cl_2 layered with hexanes. Orange rods formed overnight (100 mg, 26% yield). **7a**: IR (KBr): 1874, 1773 cm^{-1} (ν_{CO}). ^1H NMR (CD_2Cl_2, RT): δ 7.27, 7.10 (m, 3:2 H, WPMe_2*Ph*), 5.97, 5.74, 5.49 (s, 1:1:1 H, Tp′C*H*), 2.52, 2.31, 2.29, 2.27, 2.23, 1.64 (s, Tp′CH_3), 1.73 (d, 3 H, $^2J_{PH}$ = 8 Hz, WP*Me*$_2$Ph), 0.78 (d, 3 H, $^3J_{PH}$ = 4 Hz, WCH_3), 0.74 (d, 3 H, $^2J_{PH}$ = 9 Hz, WP*Me*$_2$Ph). $^{13}C\{^1H\}$ NMR (CD_2Cl_2, RT): δ 246.5 (d, $^2J_{PC}$ = 33 Hz, W*C*O), 227.4 (d, $^2J_{PC}$ = 4 Hz, W*C*O), 154.7 (d, $^3J_{PC}$ = 1 Hz, Tp′*C*CH$_3$), 152.3, 151.2, 147.0, 145.20, 145.15 (s, Tp′*C*CH$_3$), 139.0, 130.4, 129.6, 128.3 (d, 1:2:1:2 C, WPMe_2*Ph*), 107.9, 107.7, 106.8 (s, Tp′*C*H), 19.3 (d, $^1J_{PC}$ = 32 Hz, WP*Me*$_2$-Ph), 16.2, 16.0, 15.8, 13.05, 12.91, 12.86 (s, Tp′C*C*H$_3$), 12.95 (d, $^1J_{PC}$ = 33 Hz, WP*Me*$_2$Ph), 11.1 (d, $^2J_{PC}$ = 11 Hz, W*C*H$_3$). $^{31}P\{^1H\}$ NMR (CD_2Cl_2, RT): δ 0.8 (s, $^1J_{WP}$ = 230 Hz, W*P*Me$_2$-Ph).

Tp′(CO)(PMe_2Ph)W(η^2-C(O)CH_3) (7b). Crystals of **7a** were dissolved in CH_2Cl_2 or CD_2Cl_2, and η^2-acyl complex **7b** was found to be the major species in solution (**7a**:**7b** = 1:6). **7b**: IR (CH_2Cl_2): 1756 cm^{-1} (ν_{CO}). ^1H NMR (CD_2Cl_2, RT): δ 7.20, 7.16, 7.01 (m, 1:2:2 H, WPMe_2*Ph*), 5.85, 5.80, 5.38 (s, 1:1:1 H, Tp′C*H*), 2.79 (d, 3 H, $^3J_{PH}$ = 1 Hz, WC(O)CH_3), 2.47, 2.34, 2.33, 2.30, 2.00, 1.73 (s, Tp′CH_3), 1.94 (d, 3 H, $^2J_{PH}$ = 8 Hz, WP*Me*$_2$Ph), 1.38 (d, 3 H, $^2J_{PH}$ = 7 Hz, WP*Me*$_2$Ph). $^{13}C\{^1H\}$ NMR (CD_2Cl_2, RT): δ 267.0 (d, $^2J_{PC}$ = 26 Hz, W*C*(O)CH$_3$), 234.7 (d, $^2J_{PC}$ = 4 Hz, $^1J_{WC}$ = 211 Hz, W*C*O), 155.7 (d, $^3J_{PC}$ = 2 Hz, Tp′*C*CH$_3$), 152.8, 151.6, 146.7, 144.8, 144.3 (s, Tp′*C*CH$_3$), 139.6, 130.4, 128.9, 128.0 (d, 1:2:1:2 C, WPMe_2*Ph*), 107.8, 107.5, 106.5 (s, Tp′*C*H), 28.9 (s, WC(O)CH$_3$), 19.7 (d, $^1J_{PC}$ = 27 Hz, WP*Me*$_2$Ph), 18.9 (d, $^1J_{PC}$ = 28 Hz, WP*Me*$_2$Ph), 17.6, 14.6, 14.5, 13.0, 12.81, 12.79 (s, Tp′C*C*H$_3$). $^{31}P\{^1H\}$ NMR (CD_2Cl_2, RT): δ 1.8 (s, $^1J_{WP}$ = 279 Hz, W*P*Me$_2$Ph).

Tp′(CO)$_2$(PMe_2Ph)W(CH_3) (C_S) (7c). The solution prepared by dissolving crystals of **7a** in CD_2Cl_2 (vide supra) consisted primarily of **7a** and **7b** with some **7c** (**7a**:**7b**:**7c** = 7:42:1). A ^1H NMR spectrum of the same solution 3 days later revealed that the concentration of **7c** had increased such that **7a** and **7c** were approximately equal in concentration (**7a**:**7b**:**7c** = 1:6:1). The solution was monitored by ^1H NMR for a month, and no further change was detected. **7c**: IR (CD_2Cl_2): 1903, 1794 cm^{-1} (ν_{CO}). ^1H NMR (CD_2Cl_2, RT): δ 7.79, 7.41, 7.36 (m, 2:2:1 H, WPMe_2*Ph*), 5.88, 5.78 (s, 1:2 H, Tp′C*H*), 2.39 (d, 6 H, $^2J_{PH}$ = 9 Hz, WP*Me*$_2$Ph), 2.37, 2.34 (s, 9:3 H, Tp′CH_3), 1.79 (br s, 6 H, Tp′CH_3), −0.23 (d, 3 H, $^3J_{PH}$ = 10 Hz, $^2J_{WH}$ = 3 Hz, WCH_3). $^{13}C\{^1H\}$ NMR (CD_2Cl_2, RT): δ 251.4 (d, $^2J_{PC}$ = 34 Hz, W*C*O), 150.8, 150.2, 145.4, 144.4 (s, 2:1:1:2 C, Tp′*C*CH$_3$), 142.2, 131.6, 129.4, 127.6 (d, 1:2:1:2 C, WPMe_2*Ph*), 107.3, 107.1 (s, 1:2 Tp′*C*H), 19.7 (br d, based on HMQC and **7c**, WP*Me*$_2$-Ph), 15.8, 14.8, 13.2, 13.0 (s, 1:2:1:2 C, Tp′C*C*H$_3$). $^{31}P\{^1H\}$ NMR (CD_2Cl_2, RT): δ 2.9 (s, $^1J_{WP}$ = 92 Hz, W*P*Me$_2$Ph). Anal. Calcd for $C_{26}H_{36}N_6BO_2PW$: C, 45.24; H, 5.26; N, 12.18. Found: C, 45.34; H, 5.19; N, 12.18.

Tp′(CO)$_2$(PMe_3)W(CH_3) (C_1) (8a). See **7a** for the synthetic procedure. The major IR absorbance peaks in solution were initially 1897, 1793 cm^{-1}, and the minor absorbance peak was 1777 cm^{-1}. Crystals (81 mg, 25% yield) were grown from Et_2O and hexanes. Some of the crystals were dark red cubes (roughly a tenth of the crystals) that incorporated both **8a** and **8b** in a 1:1 ratio according to IR (KBr) and X-ray (vide infra). **8a**: IR (KBr): 1892, 1785 cm^{-1} (ν_{CO}). ^1H NMR (CD_2Cl_2, RT): δ 5.91, 5.86, 5.73 (s, 1:1:1 H, Tp′C*H*), 2.46, 2.43, 2.40, 2.28, 2.27, 2.23 (s, Tp′CH_3), 1.06 (d, 9 H, $^2J_{PH}$ = 9 Hz, WPMe_3), 0.67 (d, $^3J_{PH}$ = 4 Hz, WCH_3). $^{13}C\{^1H\}$ NMR (CD_2Cl_2, RT): δ 246.3 (d, $^2J_{PC}$ = 34 Hz, W*C*O), 227.9 (d, $^2J_{PC}$ = 4 Hz, W*C*O), 154.4, 152.2, 151.1, 147.2, 145.1 (s, 1:1:1:1:2 C, Tp′*C*CH$_3$), 107.9, 107.4, 106.7 (s, Tp′*C*H), 17.5 (d, $^1J_{PC}$ = 29 Hz, WP*Me*$_3$), 17.2, 16.6, 16.0, 13.2, 13.0, 12.9 (s, Tp′C*C*H$_3$), 10.3 (d, $^2J_{PC}$ = 11 Hz, W*C*H$_3$). $^{31}P\{^1H\}$ NMR (CD_2Cl_2, RT): δ 8.4 (s, $^1J_{WP}$ = 230 Hz, W*P*Me$_3$).

Tp′(CO)(PMe_3)W(η^2-C(O)CH_3) (8b). Crystals consisting of **8a** and **8b** (1:1 ratio in crystalline form) were dissolved in CD_2Cl_2, and η^2-acyl complex **8b** was found to be the major species in equilibrium with methyl complex **8a** (**8a**:**8b** = 1:4). **8b**: IR (KBr): 1752 cm^{-1} (ν_{CO}). ^1H NMR (CD_2Cl_2, RT): δ 5.86, 5.84, 5.74 (s, 1:1:1 H, Tp′C*H*), 2.81 (d, $^3J_{PH}$ = 1 Hz, WC(O)CH_3), 2.42, 2.40, 2.37, 2.301, 2.297, 1.84 (s, Tp′CH_3), 1.32 (d, $^2J_{PC}$ = 8 Hz, WP*Me*$_3$). $^{13}C\{^1H\}$ NMR (CD_2Cl_2, RT): δ 267.1 (d, $^2J_{PC}$ = 26 Hz, W*C*(O)CH$_3$), 234.3 (d, $^2J_{PC}$ = 4 Hz, W*C*O), 156.2 (d, $^3J_{PC}$ = 1 Hz, Tp′*C*CH$_3$), 152.7, 151.3, 147.1, 144.6, 144.3 (s, Tp′*C*CH$_3$), 107.7, 107.5, 106.4 (s, Tp′*C*H), 28.7 (s, WC(O)CH$_3$), 19.6 (d, $^2J_{PC}$ = 26 Hz, WP*Me*$_3$), 17.9, 14.7, 14.6, 13.3, 12.82, 12.76 (s, Tp′C*C*H$_3$). $^{31}P\{^1H\}$ NMR (CD_2Cl_2, RT): δ −11.2 (s, $^1J_{WP}$ = 285 Hz, W*P*Me$_3$).

Tp′(CO)$_2$(PMe_3)W(CH_3) (C_s) (8c). A solution prepared with crystals of **8a** and **8b** dissolved in CD_2Cl_2 (vide supra) consisted primarily of **8a** and **8b** and possessed resonance peaks for a C_s symmetric third species that were assigned to the methyl complex Tp′(CO)$_2$($PMePh_2$)W(CH_3) (**8c**) (**8a**:**8b**:**8c** = 4:16:1). A ^1H NMR spectrum of the solution a day later revealed that the concentration of **8c** had increased (**8a**:**8b**:**8c** = 1:4:4). Orange needles of **8c** formed the bulk of the crystals produced by the recrystallization described for **8a**. A solution prepared with crystals of **8c** dissolved in CH_2Cl_2 (1903, 1794 cm^{-1}) or CD_2Cl_2 consisted primarily of **8c** and only trace amounts of **8a** and **8b**. A ^1H NMR spectrum of the CD_2Cl_2 solution two weeks later revealed that the concentration of **8a** and **8b** had increased (**8a**:**8b**:**8c** = 1:4:8). **8c**: IR (KBr): 1899, 1791 cm^{-1} (ν_{CO}). ^1H NMR (CD_2Cl_2, RT): δ 5.91, 5.90 (s, 2:1 H, Tp′C*H*), 2.44, 2.41, 2.30, 2.23 (s, 6:3:3:6 H, Tp′CH_3), 2.04 (d, 9 H, $^2J_{PH}$ = 9 Hz, WP*Me*$_3$), −0.12 (d, 3 H, $^3J_{PH}$ = 10 Hz, $^2J_{WH}$ = 3 Hz, WCH_3). $^{13}C\{^1H\}$ NMR (CD_2Cl_2, RT): δ 250.1 (d, 2 C, $^2J_{PC}$ = 36 Hz, $^1J_{WC}$ = 152 Hz, W*C*O), 150.5, 145.3, 144.5 (s, 2:1:2 C), Tp′*C*CH$_3$), 150.5 (d, $^3J_{PC}$ = 3 Hz, Tp′*C*CH$_3$), 107.1 (s, 3 C, Tp′*C*H), 19.7 (br d, $^1J_{PC}$ = 40 Hz, WP*Me*$_3$), 15.8, 15.5, 13.0, 12.9 (s, 1:2:1:2 C, Tp′C*C*H$_3$), 9.1 (d, $^2J_{PC}$ = 36 Hz, $^1J_{WC}$ = 50 Hz, WCH$_3$). $^{31}P\{^1H\}$ NMR (CD_2Cl_2, RT): δ 2.0 (s, $^1J_{WP}$ = 83 Hz, W*P*Me$_3$). Anal. Calcd for $C_{21}H_{34}N_6BO_2PW$: C, 40.15; H, 5.46; N, 13.38. Found: C, 40.19; H, 5.49; N, 13.46.

Tp′(CO)($PMePh_2$)W(η^2-C(O)CH_3) (9b). See **7a** for the synthetic procedure. The first IR spectrum obtained of the THF reaction solution after addition of acid revealed absorbance peaks at 1899 and 1793 cm^{-1} (minor) and 1777 cm^{-1} (major).

Table 7. Crystal and Data Collection Parameters for Tp′(CO)$_2$(PMe_2Ph)W(CH_3) (7a) and Tp′(CO)$_2$(PMe_3)W(CH_3) (8c)

	7a	**8c**
formula	$C_{26}H_{36}N_6BO_2PW$	$C_{21}H_{34}N_6BO_2PW$
fw	690.24	628.17
color	orange	orange
cryst syst	monoclinic	monoclinic
space group	$P2_1/n$	$P2_1/c$
a, Å	11.1551(3)	12.0377(2)
b, Å	18.1380(6)	13.2617(2)
c, Å	13.9469(5)	16.3479(3)
β, deg	101.532(1)	107.8040(10)
V, Å^3	2764.93(15)	2484.80(7)
d, g/cm^3	1.658	1.679
Z	4	4
temp, K	173(2)	173(2)
R(int)	0.036	0.0536
no. of params refined	334	316
final R indices	R_f = 0.029	R_f = 0.0327
($I > 2\sigma(I)$)	R_w = 0.031	R_w = 0.0703
R indices (all data)	R_f = 0.047	R_f = 0.0752
	R_w = 0.034	R_w = 0.0888
GoF	1.2015	1.067

Table 8. Crystal and Data Collection Parameters for Tp′(CO)$_2$(PMe$_3$)W(CH$_3$) (8a) and Tp′(CO)(PMe$_3$)W(η^2-C(O)CH$_3$) (8b)

formula	$C_{21}H_{34}N_6BO_2PW$ x 2
fw	1256.33
color	red
cryst syst	monoclinic
space group	$P2_1/c$
a, Å	18.2841(4)
b, Å	18.5662(4)
c, Å	16.1972(4)
β, deg	111.822(1)
V, Å^3	5104.40(20)
d, g/cm^3	1.635
Z	4
temp, K	173
R(int)	0.033
no. of params refined	577
final *R* indices	$R_f = 0.034$
($I > 2\sigma(I)$)	$R_w = 0.036$
R indices (all data)	$R_f = 0.054$
	$R_w = 0.037$
GoF	1.6967

Following solvent removal and chromatography, red crystals consisting of **9b** (157 mg, 41% yield) were grown from CH_2Cl_2 and hexanes. A CD_2Cl_2 solution prepared from the red crystals of **9b** was found to consist of **9b** and trace amounts of **9a** and **9c**. **9b**: IR (KBr): 1758 cm^{-1} (ν_{CO}). ^{1}H NMR (CD_2Cl_2, RT): δ 7.77, 7.45 (m, 2:3 H, PMe*Ph*$_2$), 7.17, 7.07, 6.83 (m, 1:2:2 H, PMe*Ph*$_2$), 5.86, 5.80, 5.25, (s, 1:1:1 H, Tp′C*H*), 2.51, 2.40, 2.33, 2.31, 1.91, 1.51 (s, Tp′C*H*$_3$), 2.50 (d, $^3J_{PH} = 1$ Hz, WC(O)C*H*$_3$), 1.64 (d, $^2J_{PH} = 7$ Hz, WP*Me*Ph$_2$). ^{13}C{^{1}H} NMR (CD_2Cl_2, RT): δ 267.6 (d, $^2J_{PC} = 26$ Hz, $^1J_{WC} = 44$ Hz, W*C*(O)CH$_3$), 237.3 (d, $^2J_{PC} = 4$ Hz, $^1J_{WC} = 210$ Hz, W*C*O), 155.5 (d, $^3J_{PC} = 2$ Hz, Tp′*C*CH$_3$), 153.0, 152.4, 146.5, 145.4, 144.0 (s, Tp′*C*CH$_3$), 138.7, 137.9, 134.3, 132.0, 130.2, 128.8, 128.6, 127.7 (d, 1:1:2:2:1:1:2:2 C, WPMe*Ph*$_2$), 108.1, 106.6 (s, 1:1 C, Tp′CH), 107.7 (d, $^4J_{PC} = 1$ Hz, Tp′*C*H), 28.9 (s, WC(O)*C*H$_3$), 19.0 (d, $^1J_{PC} = 28$ Hz, WP*Me*Ph$_2$), 17.9, 14.4, 14.3, 13.0, 12.9, 12.8, (s, Tp′C*C*H$_3$). ^{31}P-{^{1}H} NMR (CD_2Cl_2, RT): δ 20.8 (s, $^1J_{WP} = 275$ Hz, W*P*MePh$_2$). Anal. Calcd for $C_{31}H_{38}N_6BO_2PW$: C, 49.49; H, 5.09; N, 11.17. Found: C, 49.20; H, 5.04; N, 11.17.

X-ray Crystal Structure Determinations. Crystals of **7a**, **8a** with **8b**, and **8c** measuring 0.30 × 0.15 × 0.10 mm^3, 0.35 × 0.30 × 0.10 mm^3, and 0.30 × 0.30 × 0.10 mm^3, respectively, were placed on a Bruker SMART 1K diffractometer, and intensity data were collected by using the ω-scan mode. Data were collected in the $\pm h$, k, l quadrant for **7a**, the $\pm h$, k, l quadrant for **8a** with **8b**, and the $\pm h$, $\pm k$, $\pm l$ sphere for **8c**. The structure of **8c** contains 20% disorder that reflects rotation of the W−Me group to overlap one of the W−CO groups. Crystal and data collection parameters are listed in Tables 7 and 8.

Acknowledgment. We thank the National Science Foundation for support.

Supporting Information Available: Further crystallographic information for **7a**, **8a** with **8b**, and **8c** are available free of charge via the Internet at http://pubs.acs.org.

OM049725S